
Beyond the Signs: Nonparametric Tensor Completion via Sign Series

Anonymous Author(s)

Affiliation

Address

email

Abstract

1 We consider the problem of tensor estimation from noisy observations with possibly
2 missing entries. A nonparametric approach to tensor completion is developed
3 based on a new model which we coin as sign representable tensors. The model
4 represents the signal tensor of interest using a series of structured sign tensors.
5 Unlike earlier methods, the sign series representation effectively addresses both
6 low- and high-rank signals, while encompassing many existing tensor models—
7 including CP models, Tucker models, single index models, structured tensors with
8 repeating entries—as special cases. We provably reduce the tensor estimation
9 problem to a series of structured classification tasks, and we develop a learning
10 reduction machinery to empower existing low-rank tensor algorithms for more
11 challenging high-rank estimation. Excess risk bounds, estimation errors, and
12 sample complexities are established. We demonstrate the outperformance of our
13 approach over previous methods on two datasets, one on human brain connectivity
14 networks and the other on topic data mining.

15 1 Introduction

16 Higher-order tensors have recently received much attention in enormous fields including social
17 networks [3], neuroscience [35], and genomics [26]. Tensor methods provide effective representation
18 of the hidden structure in multiway data. In this paper we consider the signal plus noise model,
19

$$\mathcal{Y} = \Theta + \mathcal{E}, \quad (1)$$

20 where $\mathcal{Y} \in \mathbb{R}^{d_1 \times \dots \times d_K}$ is an order- K data tensor, Θ is an unknown signal tensor of interest, and \mathcal{E} is
21 a noise tensor. Our goal is to accurately estimate Θ from the incomplete, noisy observation of \mathcal{Y} . In
22 particular, we focus on the following two problems:

23 Q1 [Nonparametric tensor estimation]. How to flexibly estimate Θ under a wide range of structures,
24 including both low-rankness and high-rankness?

25 Q2 [Complexity of tensor completion]. How many observed tensor entries do we need to consistently
26 estimate the signal Θ ?

27 **Inadequacies of low-rank models.** The signal plus noise model (2) is popular in tensor literature.
28 Existing methods estimate the signal tensor based on low-rankness of Θ [27, 31]. Common low-rank
29 models include Canonical Polyadic (CP) tensors [24], Tucker tensors [11], and block tensors [37].
30 While these methods have shown great success in theory, tensors in applications often violate the
31 low-rankness. Here we provide two examples to illustrate the limitation of classical models.

32 The first example reveals the sensitivity of tensor rank to order-preserving transformations. Let
33 $\mathcal{Z} \in \mathbb{R}^{30 \times 30 \times 30}$ be an order-3 tensor with tensor rank(\mathcal{Z}) = 3 (formal definition is deferred to the
34 end of this section). Suppose a monotonic transformation $f(z) = (1 + \exp(-cz))^{-1}$ is applied to \mathcal{Z}
35 entrywise, and we let the signal Θ in model (1) be the tensor after transformation. Figure 1a plots

the numerical rank (see Appendix B.1) of Θ versus c . As we see, the rank increases rapidly with c , rendering traditional low-rank tensor methods ineffective in the presence of mild order-preserving nonlinearities. In digital processing [17] and genomics analysis [26], the tensor of interest often undergoes unknown transformation prior to measurements. The sensitivity to transformation makes the low-rank model less desirable in practice.

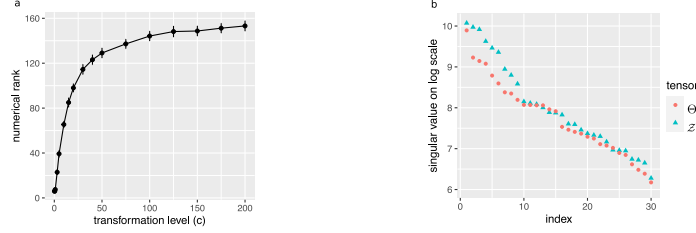


Figure 1: (a) Tensor rank vs. c in the first example. (b) Top $d = 30$ tensor singular values in the second example.

The second example demonstrates the inadequacy of classical low-rankness in representing special structures. Here we consider the signal tensor of the form $\Theta = \log(1 + Z)$, where $Z \in \mathbb{R}^{d \times d \times d}$ is an order-3 tensor with entries $Z(i, j, k) = d^{-1} \max(i, j, k)$ for $i, j, k \in \{1, \dots, d\}$. The matrix analogy of Θ was studied in graphon analysis [8]. In this case neither Θ nor Z is low-rank; in fact, the rank is no smaller than the dimension d as illustrated in Figure 1b. Again, classical low-rank models fail to address this type of tensor structure.

In the above and many other examples, the signal tensors Θ of interest have high rank. Classical low-rank models will miss these important structures. The observations have motivated us to develop more flexible tensor modeling.

Our contributions. We develop a new model called sign representable tensors to address the aforementioned challenges. Figure 2 illustrates our main idea. Our approach is built on the sign series representation of the signal tensor, and we propose to estimate the sign tensors through a series of weighted classifications. In contrast to existing methods, our method is guaranteed to recover a wide range of low- and high-rank signals. We highlight two main contributions that set our work apart from earlier literature.

Statistically, the problem of high-rank tensor estimation is challenging. Existing estimation theory [3, 31, 7] exclusively focuses on the regime of fixed r growing d . However, such premise fails in high-rank tensors, where the rank may grow with, or even exceed, the dimension. A proper notion of nonparametric complexity is crucial. We show that, somewhat surprisingly, the sign tensor series not only preserves all information in the original signals, but also brings the benefits of flexibility and accuracy over classical low-rank models. The results fill the gap between parametric (low-rank) and nonparametric (high-rank) tensors, thereby greatly enriching the tensor model literature.

Computationally, a number of polynomial-time algorithms are readily available for 1-bit tensor estimation [36, 20, 17]. These algorithms enjoy computational efficiency while being restricted to binary inputs. Our work is orthogonal to these algorithm development, and we show that the high-rank tensor estimate is provably reducible to a series of binary tensor problems with carefully-designed weights. This reduction provides a generic engine to empower existing algorithms for a wider range of structured tensor problems. We use a divide-and-concur approach to combine efficient base algorithms, thereby achieving computational accuracy without the need to reinvent the wheel. The flexibility to import and adapt existing tensor algorithms is one advantage of our method.

We also highlight the challenges associated with tensors compared to matrices. High-rank matrix estimation is recently studied under nonlinear models [15] and subspace clustering [32, 13]. However, high-rank tensor problems is more challenging, because the tensor rank often exceeds the dimension when order K greater than two [4]. This is in sharp contrast to matrices ($K = 2$). We show that, applying matrix methods to higher-order tensors results in suboptimal estimates. A full exploitation of the higher-order structure is needed; this is another challenge we address in this paper.

Notation. We use $[n] = \{1, \dots, n\}$ for n -set with $n \in \mathbb{N}_+$, $a_n \lesssim b_n$ if $\lim_{n \rightarrow \infty} a_n/b_n \leq c$ for some constant $c > 0$, and $a_n \asymp b_n$ if $c_1 \leq \lim_{n \rightarrow \infty} a_n/b_n \leq c_2$ for some constants $c_1, c_2 > 0$. We use $\mathcal{O}(\cdot)$ to denote the big-O notation, $\tilde{\mathcal{O}}(\cdot)$ the variant hiding logarithmic factors. Let $\Theta \in \mathbb{R}^{d_1 \times \dots \times d_K}$ denote an order- K (d_1, \dots, d_K)-dimensional tensor, and $\Theta(\omega) \in \mathbb{R}$ denote the tensor entry indexed by $\omega \in [d_1] \times \dots \times [d_K]$. An event A is said to occur “with very high probability” if $\mathbb{P}(A)$ tends to 1

82 faster than any polynomial of tensor dimension $d := \min_k d_k \rightarrow \infty$. The tensor rank [24] is defined
83 by $\text{rank}(\Theta) = \min\{r \in \mathbb{N}: \Theta = \sum_{s=1}^r \mathbf{a}_s^{(1)} \otimes \cdots \otimes \mathbf{a}_s^{(K)}\}$, where $\mathbf{a}_s^{(k)} \in \mathbb{R}^{d_k}$ are vectors for
84 $k \in [K], s \in [r]$, and \otimes denotes the outer product of vectors. We use $\text{sgn}(\cdot): \mathbb{R} \rightarrow \{-1, 1\}$ to denote
85 the sign function, where $\text{sgn}(y) = 1$ if $y \geq 0$ and -1 otherwise. We allow univariate functions, such
86 as $\text{sgn}(\cdot)$ and general $f: \mathbb{R} \rightarrow \mathbb{R}$, to be applied to tensors in an element-wise manner.

87 2 Model and proposal overview

88 Let \mathcal{Y} be an order- K (d_1, \dots, d_K) -dimensional tensor generated from the model

$$\mathcal{Y} = \Theta + \mathcal{E}, \quad (2)$$

89 where $\Theta \in \mathbb{R}^{d_1 \times \cdots \times d_K}$ is an unknown signal tensor, and \mathcal{E} is a noise tensor consisting of zero-mean,
90 independent but not necessarily identically distributed entries. We allow heterogenous noise, in
91 that the marginal distribution of noise entry $\mathcal{E}(\omega)$ may depend on ω . For a cleaner exposition, we
92 assume the noise is bounded and the range of Y is in $[-1, 1]$; the extension to a sub-Gaussian noise
93 is provided in Appendix B.3. Our observation is an incomplete data tensor from (2), denoted \mathcal{Y}_Ω ,
94 where $\Omega \subset [d_1] \times \cdots \times [d_K]$ is the index set of observed entries. We consider a general model on Ω
95 that allows both uniform and non-uniform samplings. Specifically, let $\Pi = \{p_\omega\}$ be an arbitrarily
96 predefined probability distribution over the full index set with $\sum_{\omega \in [d_1] \times \cdots \times [d_K]} p_\omega = 1$. We use
97 $\omega \sim \Pi$ to denote the sampling rule, meaning ω in Ω are i.i.d. draws with replacement from distribution
98 Π . The goal is to estimate Θ from \mathcal{Y}_Ω . Note that Θ is not necessarily low-rank.

99 **Proposal intuition.** Before describing our main results, we provide the intuition behind our method.
100 In the two examples in Section 1, the high-rankness in the signal Θ makes the estimation challenging.
101 Now let us examine the sign of the π -shifted signal $\text{sgn}(\Theta - \pi)$ for any given $\pi \in [-1, 1]$. It
102 turns out that, these sign tensors share the same sign patterns as low-rank tensors. Indeed, the
103 signal tensor in the first example has the same sign pattern as a rank-4 tensor, since $\text{sgn}(\Theta - \pi) =$
104 $\text{sgn}(\mathcal{Z} - f^{-1}(\pi))$. The signal tensor in the second example has the same sign pattern as a rank-2
105 tensor, since $\text{sgn}(\Theta(i, j, k) - \pi) = \text{sgn}(\max(i, j, k) - d(e^\pi - 1))$ (see Example 5 in Section 3).

106 The above observation suggests a general framework to estimate both low- and high-rank signal
107 tensors. Figure 2 illustrates the main crux of our method. We propose to estimate the signal tensor Θ
108 by taking the average over structured sign tensors

$$\hat{\Theta} = \frac{1}{2H+1} \sum_{\pi \in \mathcal{H}} \text{sgn}(\hat{\mathcal{Z}}_\pi), \text{ where } \hat{\mathcal{Z}}_\pi = \arg \min_{\text{low rank tensor } \mathcal{Z}} \text{Weighted-Loss}(\text{sgn}(\mathcal{Z}), \text{sgn}(\mathcal{Y}_\Omega - \pi)). \quad (3)$$

109 Here $\text{sgn}(\hat{\mathcal{Z}}_\pi) \in \{-1, 1\}^{d_1 \times \cdots \times d_K}$ is the sign tensor estimated at a series of $\pi \in \mathcal{H} = \{-1, \dots,$
110 $-1/H, 0, 1/H, \dots, 1\}$, and $\text{Weighted-Loss}(\cdot, \cdot)$ denotes a classification objective function with an
111 entry-specific weight to each tensor entry; its specific form will be described in Section 3.2. To obtain
112 $\text{sgn}(\hat{\mathcal{Z}}_\pi)$ for a given π , we propose to dichotomize the data tensor into a sign tensor $\text{sgn}(\mathcal{Y}_\Omega - \pi)$ and
113 estimate the de-noised sign by performing weighted classification.

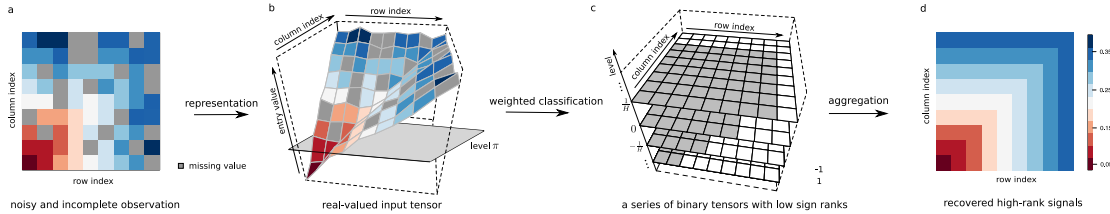


Figure 2: Illustration of our method in the context of an order-2 tensor (a.k.a. matrix). (a): a noisy, incomplete tensor input. (b)-(c): Estimation of sign tensor series $\text{sgn}(\Theta - \pi)$ for $\pi \in \{-1, \dots, -1/H, 0, 1/H, \dots, 1\}$. (d): recovered signal $\hat{\Theta}$. The depicted signal is a full-rank matrix based on Example 5 in Section 3.

114 Our approach is built on the nonparametric sign representation of signal tensors. We show that a
115 careful aggregation of dichotomized data not only preserves all information in the original signals,
116 but also brings benefits of accuracy and flexibility over classical low-rank models. Unlike traditional
117 methods, the sign representation is guaranteed to recover both low- and high-rank signals. In addition,
118 a total of $H = \text{poly}(d)$ dichotomized problems suffice to recover Θ under the considered model. The
119 method therefore enjoys both statistical effectiveness and computational efficiency.

3 Oracle properties of sign representable tensors

This section develops sign representable tensor models for Θ in (2). We characterize the algebraic and statistical properties of sign tensor series, which serves the foundation for our method.

3.1 Sign-rank and sign tensor series

Let Θ be the tensor of interest, and $\text{sgn}(\Theta)$ the corresponding sign pattern. The sign patterns induce an equivalence relationship between tensors. Two tensors are called sign equivalent, denoted \simeq , if they have the same sign pattern.

Definition 1 (Sign-rank). The sign-rank of a tensor $\Theta \in \mathbb{R}^{d_1 \times \dots \times d_K}$ is defined by the minimal rank among all tensors that share the same sign pattern as Θ ; i.e.,

$$\text{srnk}(\Theta) = \min\{\text{rank}(\Theta') : \Theta' \simeq \Theta, \Theta' \in \mathbb{R}^{d_1 \times \dots \times d_K}\}.$$

This concept is important in combinatorics [10], complexity theory [1], and quantum mechanics [12]; we extend the notion to continuous-valued tensors. Note that the sign-rank concerns only the sign pattern but discards the magnitude information of Θ . In particular, $\text{srnk}(\Theta) = \text{srnk}(\text{sgn}(\Theta))$.

Like most tensor problems [23], determining the sign-rank is NP hard in the worst case [1]. Fortunately, tensors arisen in applications often possess special structures that facilitate analysis. The sign-rank is upper bounded by tensor rank. More generally, we show the following properties.

Proposition 1 (Upper bounds of the sign-rank).

(a) [Upper bounds] For any strictly monotonic function $g: \mathbb{R} \rightarrow \mathbb{R}$ with $g(0) = 0$, we have $\text{srnk}(\Theta) \leq \text{rank}(g(\Theta))$.

(b) [Broadness] For every order $K \geq 2$ and dimension d , there exist tensors $\Theta \in \mathbb{R}^{d \times \dots \times d}$ such that $\text{rank}(\Theta) \geq d$ but $\text{srnk}(\Theta - \pi) \leq 2$ for all $\pi \in \mathbb{R}$.

Propositions 1 demonstrates the strict broadness of low sign-rank family over the usual low-rank family. In particular, the sign-rank can be much smaller than the tensor rank, as we have shown in the two examples of Section 1. We provide several additional examples in Appendix B.2 in which the tensor rank grows with dimension d but the sign-rank remains a constant. The results highlight the advantages of using sign-rank in the high-dimensional tensor analysis.

We now introduce a tensor family, which we coin as “sign representable tensors”.

Definition 2 (Sign representable tensors). Fix a level $\pi \in [-1, 1]$. A tensor Θ is called (r, π) -sign representable, if the tensor $(\Theta - \pi)$ has sign-rank bounded by r . A tensor Θ is called r -sign (globally) representable, if Θ is (r, π) -sign representable for all $\pi \in [-1, 1]$. The collection $\{\text{sgn}(\Theta - \pi) : \pi \in [-1, 1]\}$ is called the sign tensor series. We use $\mathcal{P}_{\text{sgn}}(r) = \{\Theta : \max_{\pi \in [-1, 1]} \text{srnk}(\Theta - \pi) \leq r\}$ to denote the r -sign representable tensor family.

We next show that the r -sign representable tensor family is a general model that incorporates most existing tensor models, including low-rank tensors, single index models, GLM models, and structured tensors with repeating entries.

Example 1 (CP/Tucker low-rank models). The CP and Tucker low-rank tensors are the two most popular tensor models [28]. Let Θ be a low-rank tensor with CP rank r . We see that Θ belongs to the sign representable family; i.e., $\Theta \in \mathcal{P}_{\text{sgn}}(r + 1)$ (the constant 1 is due to $\text{rank}(\Theta - \pi) \leq r + 1$). Similar results hold for Tucker low-rank tensors $\Theta \in \mathcal{P}_{\text{sgn}}(r + 1)$, where $r = \prod_k r_k$ with r_k being the k -th mode Tucker rank of Θ .

Example 2 (Tensor block models (TBMs)). Tensor block model [37, 9] assumes a checkerboard structure among tensor entries under marginal index permutation. The signal tensor Θ takes at most r distinct values, where r is the total number of multiway blocks. Our model incorporates TBM because $\Theta \in \mathcal{P}_{\text{sgn}}(r)$.

Example 3 (Generalized linear models (GLMs)). Let \mathcal{Y} be a binary tensor from a logistic model [36] with mean $\Theta = \text{logit}(\mathcal{Z})$, where \mathcal{Z} is a latent low-rank tensor. Notice that Θ itself may be high-rank (see Figure 1a). By definition, Θ is a low-rank sign representable tensor. Same conclusion holds for general exponential-family models with a (known) link function [25].

Example 4 (Single index models (SIMs)). Single index model is a flexible semiparametric model proposed in economics [33] and high-dimensional statistics [5, 14]. The SIM assumes the existence of a (unknown) monotonic function $g: \mathbb{R} \rightarrow \mathbb{R}$ such that $g(\Theta)$ has rank r . We see that Θ belongs to the sign representable family; i.e., $\Theta \in \mathcal{P}_{\text{sgn}}(r + 1)$.

Example 5 (Structured tensors with repeating entries). Here we revisit the model introduced in Figure 1b of Section 1. Let Θ be an order- K tensor with entries $\Theta(i_1, \dots, i_K) = \log(1 + \max_k x_{i_k}^{(k)})$, where $x_{i_k}^{(k)}$ are given numbers in $[0, 1]$ for all $i_k \in [d_k], k \in [K]$. We conclude that $\Theta \in \mathcal{P}_{\text{sgn}}(2)$, because the sign tensor $\text{sgn}(\Theta - \pi)$ with an arbitrary $\pi \in (0, \log 2)$ is a block tensor with at most two blocks (see Figure 2c). Similar results extend to structured tensors with entries $\Theta(i_1, \dots, i_K) = g(\max_k x_{i_k}^{(k)})$, where $g(\cdot)$ is a polynomial of degree r . In this case, Θ is a high-rank tensor with at most d_{\max} distinct entries but we have $\Theta \in \mathcal{P}_{\text{sgn}}(2r)$ (see proofs in Appendix B.2).

3.2 Statistical characterization of sign tensors via weighted classification

We now provide the explicit form of the weighted loss introduced in (3), and show that sign tensors are characterized by weighted classification. The results bridge the algebraic and statistical properties of sign representable tensors.

For a given $\pi \in [-1, 1]$, define a π -shifted data tensor $\bar{\mathcal{Y}}_\Omega$ with entries $\bar{\mathcal{Y}}(\omega) = (\mathcal{Y}(\omega) - \pi)$ for $\omega \in \Omega$. We propose a weighted classification objective function

$$L(\mathcal{Z}, \bar{\mathcal{Y}}_\Omega) = \frac{1}{|\Omega|} \sum_{\omega \in \Omega} \underbrace{|\bar{\mathcal{Y}}(\omega)|}_{\text{weight}} \times \underbrace{|\text{sgn} \mathcal{Z}(\omega) - \text{sgn} \bar{\mathcal{Y}}(\omega)|}_{\text{classification loss}}, \quad (4)$$

where $\mathcal{Z} \in \mathbb{R}^{d_1 \times \dots \times d_K}$ is the decision variable to be optimized, $|\bar{\mathcal{Y}}(\omega)|$ is the entry-specific weight equal to the distance from the tensor entry to the target level π . The entry-specific weights incorporate the magnitude information into classification, where entries far away from the target level are penalized more heavily in the objective. In the special case of binary tensor $\mathcal{Y} \in \{-1, 1\}^{d_1 \times \dots \times d_K}$ and target level $\pi = 0$, the loss (4) reduces to usual classification loss.

Our proposed weighted classification function (4) is important for characterizing $\text{sgn}(\Theta - \pi)$. Define the weighted classification risk

$$\text{Risk}(\mathcal{Z}) = \mathbb{E}_{\mathcal{Y}_\Omega} L(\mathcal{Z}, \bar{\mathcal{Y}}_\Omega), \quad (5)$$

where the expectation is taken with respect to \mathcal{Y}_Ω under model (2) and the sampling distribution $\omega \sim \Pi$. The form of $\text{Risk}(\cdot)$ implicitly depends on π ; we suppress π when no confusion arises.

Proposition 2 (Global optimum of weighted risk). *Suppose the data \mathcal{Y}_Ω is generated from model (2) with $\Theta \in \mathcal{P}_{\text{sgn}}(r)$. Then, for all $\bar{\Theta}$ that are sign equivalent to $\text{sgn}(\Theta - \pi)$,*

$$\text{Risk}(\bar{\Theta}) = \inf\{\text{Risk}(\mathcal{Z}) : \mathcal{Z} \in \mathbb{R}^{d_1 \times \dots \times d_K}\} = \inf\{\text{Risk}(\mathcal{Z}) : \text{rank}(\mathcal{Z}) \leq r\}.$$

The results show that the sign tensor $\text{sgn}(\Theta - \pi)$ optimizes the weighted classification risk. This fact suggests a practical procedure to estimate $\text{sgn}(\Theta - \pi)$ via empirical risk optimization of $L(\mathcal{Z}, \bar{\mathcal{Y}}_\Omega)$. In order to establish the recovery guarantee, we shall address the uniqueness (up to sign equivalence) for the optimizer of $\text{Risk}(\cdot)$. The local behavior of Θ around π plays a key role in the accuracy.

Some additional notation is needed for stating the results in full generality. Let $d_{\text{total}} = \prod_{k=1}^K d_k$ denote the total number of tensor entries, and $\Delta s = 1/d_{\text{total}}$ a small tolerance. We quantify the distribution of tensor entries $\Theta(\omega)$ using a pseudo density, i.e., histogram with bin width $2\Delta s$. Let $G(\pi) := \mathbb{P}_{\omega \sim \Pi}[\Theta(\omega) \leq \pi]$ denote the cumulative distribution function (CDF) of $\Theta(\omega)$ under $\omega \sim \Pi$. We partition $[-1, 1] = \mathcal{N}^c \cup \mathcal{N}$, such that the pseudo density based on 2Δ -bin is uniformly bounded over \mathcal{N}^c ; i.e.,

$$\mathcal{N}^c = \left\{ \pi \in [-1, 1] : \frac{G(\pi + \Delta s) - G(\pi - \Delta s)}{\Delta s} \leq C \right\}, \text{ for some universal constant } C > 0,$$

and \mathcal{N} otherwise. Both Θ and its induced CDF G implicitly depend on the tensor dimension.

Assumption 1 (α -smoothness). Fix $\pi \in \mathcal{N}^c$. Assume there exist constants $\alpha = \alpha(\pi) > 0, c = c(\pi) > 0$, independent of tensor dimension, such that,

$$\sup_{\Delta s \leq t < \rho(\pi, \mathcal{N})} \frac{G(\pi + t) - G(\pi - t)}{t^\alpha} \leq c, \quad (6)$$

where $\rho(\pi, \mathcal{N}) := \min_{\pi' \in \mathcal{N}} |\pi - \pi'| + \Delta s$ denotes the adjusted distance from π to the nearest point in \mathcal{N} . The largest possible $\alpha = \alpha(\pi)$ in (6) is called the smoothness index at level π . We make the convention that $\alpha = \infty$ if the numerator in (6) is zero. A tensor Θ is called α -globally smooth, if (6) holds with global constants $\alpha > 0, c > 0$ for all $\pi \in \mathcal{N}^c$.

The smoothness index α quantifies the intrinsic hardness of recovering $\text{sgn}(\Theta - \pi)$ from $\text{Risk}(\cdot)$. The value of α depends on both the sampling distribution $\omega \sim \Pi$ and the behavior of $\Theta(\omega)$. The recovery is easier at levels where points are less concentrated around π with a large value of $\alpha > 1$, or equivalently, when $G(\pi)$ remains almost flat around π . A small value of $\alpha < 1$ indicates the nonexistent (infinite) density at level π , or equivalently, when the $G(\pi)$ jumps by greater than the tolerance Δs at π . Table 1 illustrates the $G(\pi)$ for various models of Θ (see Section 5).

We now reach the main theorem in this section. For two tensors Θ_1, Θ_2 , define the mean absolute error (MAE) as $\text{MAE}(\Theta_1, \Theta_2) = \mathbb{E}_{\omega \sim \Pi} |\Theta_1(\omega) - \Theta_2(\omega)|$.

Theorem 1 (Identifiability). *Assume $\Theta \in \mathcal{P}_{\text{sgn}}(r)$ is α -globally smooth. Then, for all $\pi \in \mathcal{N}^c$ and tensors $\bar{\Theta} \simeq \text{sgn}(\Theta - \pi)$, we have*

$$\text{MAE}(\text{sgn}\mathcal{Z}, \text{sgn}\bar{\Theta}) \lesssim C(\pi) [\text{Risk}(\mathcal{Z}) - \text{Risk}(\bar{\Theta})]^{\alpha/(\alpha+1)} + \Delta s, \quad \text{for all } \mathcal{Z} \in \mathbb{R}^{d_1 \times \dots \times d_K},$$

where $C(\pi) > 0$ is independent of \mathcal{Z} .

The result establishes the recovery stability of sign tensors $\text{sgn}(\Theta - \pi)$ using optimization with population risk (5). The bound immediately shows the uniqueness of the optimizer for $\text{Risk}(\cdot)$ up to a Δs -measure set under Π . We find that a higher value of α implies more stable recovery, as intuition would suggest. Similar results hold for optimization with sample risk (4) (see Section 4).

We conclude this section by applying Assumption 1 to the examples described in Section 3.1. For simplicity, suppose Π is the uniform sampling. The tensor block model is ∞ -globally smooth. This is because the set \mathcal{N} consists of finite $2\Delta s$ -bin's covering the distinct block means in Θ . Furthermore, we have $\alpha = \infty$ for all $\pi \in \mathcal{N}^c$, since the numerator in (6) is zero. Similarly, the high-rank (d, d, d) -dimensional tensor $\Theta(i, j, k) = \log(1 + \frac{1}{d} \max(i, j, k))$ is ∞ -globally smooth because $\alpha = \infty$ for all π except those in \mathcal{N} , where \mathcal{N} collects d many $2\Delta s$ -bin's covering $\log(1 + i/d)$ for all $i \in [d]$.

4 Nonparametric tensor completion via sign series

In previous sections we have established the sign series representation and its relationship to classification. In this section, we present our learning reduction proposal in details (Figure 2). We provide the estimation error bound and address the empirical implementation of the method.

4.1 Statistical error and sample complexity

Given a noisy incomplete tensor observation \mathcal{Y}_Ω from model (2), we cast the problem of estimating Θ into a series of weighted classifications. Specifically, we propose the signal tensor estimate using averaged structured sign tensors

$$\hat{\Theta} = \frac{1}{2H+1} \sum_{\pi \in \mathcal{H}} \text{sgn}\hat{\mathcal{Z}}_\pi, \quad \text{with} \quad \hat{\mathcal{Z}}_\pi = \arg \min_{\mathcal{Z}: \text{rank}\mathcal{Z} \leq r} L(\mathcal{Z}, \mathcal{Y}_\Omega - \pi), \quad (7)$$

where $\mathcal{H} = \{-1, \dots, -1/H, 0, 1/H, \dots, 1\}$ is the series of levels to aggregate, $L(\cdot, \cdot)$ denotes the weighted classification objective defined in (4), and the rank constraint on \mathcal{Z} follows from Proposition 2. For the theory, we assume the true r is known; in practice, r could be chosen in a data adaptive fashion via cross-validation or elbow method [21].

The next theorem establishes the statistical convergence for the sign tensor estimate (7).

Theorem 2 (Sign tensor estimation). *Suppose $\Theta \in \mathcal{P}_{\text{sgn}}(r)$ and $\Theta(\omega)$ is α -globally smooth under $\omega \sim \Pi$. Let $\hat{\mathcal{Z}}_\pi$ be the estimate in (7), $d = \max_{k \in [K]} d_k$, and $t_d = \frac{dr \log |\Omega|}{|\Omega|} \lesssim 1$. Then, for all $\pi \in \mathcal{N}^c$, with very high probability over \mathcal{Y}_Ω ,*

$$\text{MAE}(\text{sgn}\hat{\mathcal{Z}}_\pi, \text{sgn}(\Theta - \pi)) \lesssim t_d^{\alpha/(\alpha+2)} + \frac{1}{\rho^2(\pi, \mathcal{N})} t_d. \quad (8)$$

Theorem 2 provides the error bound for the sign tensor estimation. Compared to the population results in Theorem 1, we explicitly reveal the dependence of accuracy on the sample complexity and the level π . The result demonstrates the polynomial decay of sign errors with $|\Omega|$. Our sign estimate achieves consistent recovery using as few as $\tilde{O}(dr)$ noisy entries.

Recall that \mathcal{N} collects the levels for which the sign tensor is possibly nonrecoverable. Let $|\mathcal{N}|$ be the covering number of \mathcal{N} with $2\Delta s$ -bin's, i.e., $|\mathcal{N}| = \lceil \text{Leb}(\mathcal{N})/2\Delta s \rceil$, where $\text{Leb}(\cdot)$ is the Lebesgue

measure and $\lceil \cdot \rceil$ is the ceiling function. Combining the sign representability of the signal tensor and the sign estimation accuracy, we obtain our main results on nonparametric tensor estimation.

Theorem 3 (Tensor estimation error). *Consider the same conditions of Theorem 2. Let $\hat{\Theta}$ be the estimate in (7). For any resolution parameter $H \in \mathbb{N}_+$, with very high probability over \mathcal{Y}_Ω ,*

$$\text{MAE}(\hat{\Theta}, \Theta) \lesssim (t_d \log H)^{\frac{\alpha}{\alpha+2}} + \frac{1 + |\mathcal{N}|}{H} + t_d H \log H. \quad (9)$$

In particular, setting $H = (1 + |\mathcal{N}|)^{1/2} t_d^{-1/2} \asymp \text{poly}(d)$ yields the tightest upper bound in (9).

Theorem 3 demonstrates the convergence rate of our tensor estimation. The bound (9) reveals three sources of errors: the estimation error for sign tensors, the bias from sign series representations, and the variance thereof. The resolution parameter H controls the bias-variance tradeoff. We remark that the signal estimation error (9) is generally no better than the corresponding sign error (8). This is to be expected, since magnitude estimation is a harder problem than sign estimation.

In the special case of full observation with equal dimension $d_1 = \dots = d_K = d$ and bounded $|\mathcal{N}| \leq C$, our signal estimate achieves convergence

$$\text{MAE}(\hat{\Theta}, \Theta) \lesssim r d^{-(K-1) \min(\frac{\alpha}{\alpha+2}, \frac{1}{2})} \log^2 d,$$

by setting $H \asymp d^{(K-1)/2}$. Compared to earlier methods, our estimation accuracy applies to both low- and high-rank signal tensors. The rate depends on the sign complexity $\Theta \in \mathcal{P}_{\text{sgn}}(r)$, and this r is often much smaller than the usual tensor rank (see Section 3.1). Our result also reveals that the convergence becomes favorable as the order of data tensor increases.

We apply our method to the main examples in Section 3.1, and compare the results with existing literature. The numerical comparison is provided in Section 5.

Example 2 (TBMs). Consider a tensor block model with r multiway blocks. Our result implies a rate $\tilde{\mathcal{O}}(d^{-(K-1)/2})$ by taking $\alpha = \infty$ and $|\mathcal{N}| \leq r^K \lesssim \mathcal{O}(1)$. This rate agrees with the previous root-mean-square error (RMSE) for block tensor estimation [37].

Example 3 (GLMs). Consider a GLM tensor $\Theta = g(\mathcal{Z})$, where g is a known link function and \mathcal{Z} is a latent low-rank tensor. Suppose the CDF of $\Theta(\omega)$ is uniformly bounded as $d \rightarrow \infty$. Applying our results with $\alpha = 1$ and finite $|\mathcal{N}|$ yields $\tilde{\mathcal{O}}(d^{-(K-1)/3})$. This rate is slightly slower than the parametric RMSE rate [39, 36], as expected. The reason is that our estimate remains valid for unknown g and general high-rank tensors. The nonparametric rate is the price one has to pay for not knowing the form $\Theta = g(\mathcal{Z})$ a priori.

Example 4 (SIMs). The earlier example has shown the nonparametric rate $\tilde{\mathcal{O}}(d^{-(K-1)/3})$ when applying our method to single index tensor model. In the matrix case with $K = 2$, our result yields error rate $\tilde{\mathcal{O}}(d^{-1/3})$, which is faster than the RMSE rate $\mathcal{O}(d^{-1/4})$ obtained by [15].

Example 5 (Structured tensors with repeating entries). We consider a more general model than that in Section 1. Consider a r -sign representable tensor $\Theta \in \mathcal{P}_{\text{sgn}}(r)$ with at most d distinct entries with repetition pattern. Applying our results with $\alpha = \infty$ and $|\mathcal{N}| = d$ yields the rate $\tilde{\mathcal{O}}(d^{-(K-2)/2})$.

The following corollary reveal the sample complexity for nonparametric tensor completion.

Corollary 1 (Sample complexity for nonparametric completion). *Assume the same conditions of Theorem 3 and bounded $|\mathcal{N}|$. Then, with high probability over \mathcal{Y}_Ω ,*

$$\text{MAE}(\hat{\Theta}, \Theta) \rightarrow 0, \quad \text{as} \quad \frac{|\Omega|}{dr \log^2 |\Omega|} \rightarrow \infty.$$

Our result improves earlier work [38, 18, 29] by allowing both low- and high-rank signals. Interestingly, the sample requirements depend only on the sign complexity dr but not the nonparametric complexity α . Note that $\tilde{\mathcal{O}}(dr)$ roughly matches the degree of freedom of sign tensors, suggesting the optimality of our sample requirements.

4.2 Implementation via learning reduction

This section addresses the practical implementation of our estimation (7). We take a learning reduction approach by dividing the full procedure into a meta algorithm and $2H + 1$ base algorithms. The

Algorithm 1 Nonparametric tensor completion via learning reduction

Input: Noisy and incomplete data tensor \mathcal{Y}_Ω , rank r , resolution parameter H , ridge penalty λ .
1: **for** $\pi \in \mathcal{H} = \{-1, \dots, -\frac{1}{H}, 0, \frac{1}{H}, \dots, 1\}$ **do**
2: Define π -shifted tensor $\bar{\mathcal{Y}} = \mathcal{Y} - \pi$ and corresponding sign tensor $\text{sgn}(\bar{\mathcal{Y}}) = \text{sgn}(\mathcal{Y} - \pi)$.
3: Perform 1-bit tensor estimation algorithm [17, 36, 25, 2] on $\bar{\mathcal{Y}}_\Omega$ and obtain $\hat{\mathcal{Z}}_\pi \leftarrow \arg \min_{\text{low-rank } \mathcal{Z}} \sum_{\omega \in \Omega} |\bar{\mathcal{Y}}(\omega)| F(\mathcal{Z}(\omega) \text{sgn} \bar{\mathcal{Y}}(\omega)) + \lambda \|\mathcal{Z}\|_F^2$ where $F(\cdot)$ is the large-margin loss.
4: **end for**
Output: Estimated signal tensor $\hat{\Theta}_F = \frac{1}{2H+1} \sum_{\pi \in \mathcal{H}} \text{sgn}(\hat{\mathcal{Z}}_\pi)$.

meta algorithm takes the average of $(2H + 1) \asymp \text{poly}(d)$ sign tensors, whereas each base algorithm estimates the tensor $\text{sgn}(\Theta - \pi)$ given binary input $\text{sgn}(\mathcal{Y} - \pi)$ and a target rank r . The full procedure is described in Algorithm 1 and Figure 2.

The base algorithm reduces to a low-rank 1-bit tensor estimation problem. Following the common practice in classification [6], we replace the 0-1 loss $\ell(z, y) = |\text{sgn} z - \text{sgn} y|$ in (4) with a continuous large-margin loss $F(m)$ where $m = z \text{sgn}(y)$ is the margin. Examples of large-margin loss are hinge loss $F(m) = (1 - m)_+$, logistic loss $F(m) = \log(1 + e^{-m})$, and ψ -loss $F(m) = 2 \min(1, (1 - m)_+)$ with $m_+ = \max(m, 0)$. A number of polynomial-time algorithms with convergence guarantees are readily available for this problem [17, 36, 25, 2]. We implement hinge loss [2, 16, 22] which maintains desirable statistical properties as in 0-1 loss, because of the linear excess risk bound [34]

$$\text{Risk}(\mathcal{Z}) - \text{Risk}(\Theta - \pi) \leq C[\text{Risk}_F(\mathcal{Z}) - \text{Risk}_F(\Theta - \pi)], \quad \text{for all } \pi \in [-1, 1] \text{ and all tensor } \mathcal{Z}.$$

Here $\text{Risk}_F(\cdot)$ is defined similarly as in (5) with hinge loss in place of 0-1 loss. The resulting estimate enjoys both statistical and computational efficiency under mild conditions (see Appendix A.5).

Theorem 4 (Large-margin loss). *Let $\hat{\Theta}_F$ be the output from Algorithm 1 with F being the hinge loss. Under the set-up of Theorem 2 and technical assumptions on base algorithms, $\hat{\Theta}_F$ has the same error bound as in (9). Furthermore, the total complexity is within a $\text{poly}(d)$ factor of base algorithms.*

In principle, users can choose their own favorite large-margin losses, as long as the base algorithms are sample efficient. The comparison between various large-margin losses has been studied before [6]. Note that, instead of using $\hat{\mathcal{Z}}_\pi$ as in existing 1-bit tensor algorithms [17, 36], we use $\text{sgn}(\hat{\mathcal{Z}}_\pi)$ for more challenging nonparametric estimation. The sign aggregation brings the benefits of flexibility and accuracy over classical low-rank models.

5 Numerical experiments

Finite-sample accuracy. We compare our nonparametric tensor method (**NonparaT**) with two alternative approaches: low-rank tensor CP decomposition (**CPT**), and the matrix version of our method applied to tensor unfolding (**NonparaM**). The performance is assessed under both complete and incomplete observations. We generate signal tensors based on four models summarized in Table 1, including block tensors, transformed low rank tensors, and structured tensors with repeating entries. We consider order-3 tensors of equal dimension, and set $d \in \{15, 20, \dots, 55, 60\}$, $r \in \{2, 3, \dots, 10\}$, $H = 10 + (d - 15)/5$ in Algorithm 1. All summary statistics are averaged across 30 replicates.

Table 1: Simulation models. Here $\mathbf{M}_k \in \{0, 1\}^{d \times 3}$ denotes membership matrix, $\mathcal{C} \in \mathbb{R}^{3 \times 3 \times 3}$ the block means, $\mathbf{a} = (1, 2, \dots, d)^T/d$, \mathcal{Z}_{\max} and \mathcal{Z}_{\min} are order-3 tensors with entries $d^{-1} \max(i, j, k)$ and $d^{-1} \min(i, j, k)$.




Simulation	Signal Tensor Θ	Rank	Sign Rank	α	$ \mathcal{N} $	CDF of Tensor Entries	Noise
1	$\mathcal{C} \times \mathbf{M}_1 \times \mathbf{M}_2 \times \mathbf{M}_3$	3^3	$\leq 3^3$	∞	$\leq 3^3$		Uniform $[-0.3, 0.3]$
2	$[\mathbf{a} \otimes \mathbf{1} \otimes \mathbf{1} - \mathbf{1} \otimes \mathbf{a} \otimes \mathbf{1}]$	d	≤ 3	1	0		Normal $\mathcal{N}(0, 0.15)$
3	$\log(0.5 + \mathcal{Z}_{\max})$	$\geq d$	2	∞	d		Uniform $[-0.1, 0.1]$
4	$2.5 - \exp(\mathcal{Z}_{\min}^{1/3})$	$\geq d$	2	∞	d		Normal $\mathcal{N}(0, 0.15)$

Figure 3a-b compares the estimation error under full observation. For space consideration, only results for models 2-3 are presented in the main paper, and the rest in the Appendix C.1. We find that MAE decreases with tensor dimension for all three methods. Our method **NonparaT** achieves the best performance in all scenarios, whereas the second best method is **CPT** for model 2, and **NonparaM** for model 3. The model 2 has controlled multilinear rank along mode 3, which makes tensor methods **NonparaT** and **CPT** more accurate than **NonparaM**. The model 3 fits poorly into low-rank tensor families, and therefore, the two nonparametric methods **NonparaT** and **NonparaM** exhibit the greater

333 advantage. Figure 3c-d shows the completion error against observation fraction. We fix $d = 40$
 334 and gradually increase the observation fraction $|\Omega|/d^3$ from 0.3 to 1. Again, we find that **NonparaT**
 335 achieves the lowest error. The simulation covers a wide range of complexities, and our method shows
 336 good performance in experiments.

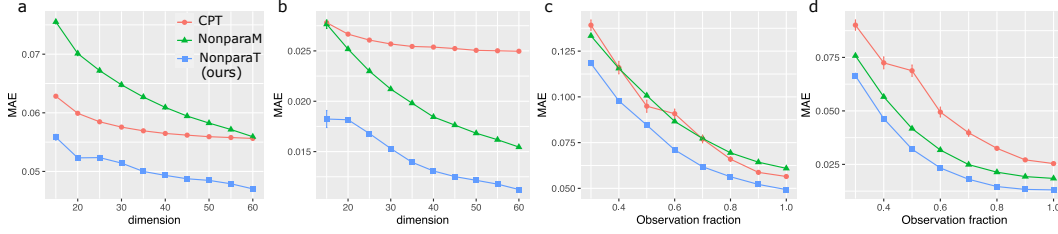


Figure 3: Performance comparison. (a)-(b): Estimation error versus tensor dimension. (c)-(d): Estimation error versus observation fraction. Panels (a) and (c) are for model 2, whereas (b) and (d) are for model 3.

337 **Data applications.** We apply our method to two tensor datasets, the MRN-114 human brain connectivity
 338 data [35], and NIPS data [19]. The brain dataset records the structural connectivity among 68
 339 brain regions for 114 individuals along with their Intelligence Quotient (IQ) scores. We organize the
 340 connectivity data into an order-3 tensor, where entries encode the presence or absence of fiber connections
 341 between brain regions across individuals. The NIPS dataset consists of word occurrence counts
 342 in papers published from 1987 to 2003. We focus on the top 100 authors, 200 most frequent words,
 343 and normalize each word count by log transformation with pseudo-count 1. The resulting dataset is
 344 an order-3 tensor with entry representing the log counts of words by authors across years.

Table 2: MAE comparison between **NonparaT** ($H = 20$) and **CPT** in the real data analysis. Standard errors are in parenthesis.

MRN-114 brain connectivity dataset			
Method	$r = 6$	$r = 9$	$r = 12$
NonparaT (Ours)	0.14(0.001)	0.12(0.001)	0.12(0.001)
CPT	0.23(0.006)	0.22(0.004)	0.21(0.006)
NIPS word occurrence dataset			
Method	$r = 6$	$r = 9$	$r = 12$
NonparaT (Ours)	0.16(0.002)	0.15(0.001)	0.14(0.001)
CPT	0.20(0.007)	0.19(0.007)	0.17(0.007)

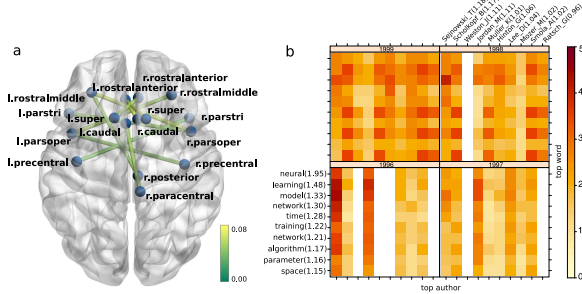


Figure 4: (a) top IQ-associated edges in the brain connectivity data. (b) top (authors, words, year) triplets in the NIPS data.

346 Table 2 compares the prediction accuracy of different methods. Reported MAEs are averaged over five
 347 runs of cross-validation, with 20% entries for testing and 80% for training. Our method substantially
 348 outperforms the low-rank CP method for every configuration under consideration. Further increment
 349 of rank appears to have little effect on the performance, and we find that increased missingness
 350 gives more advantages to our method (see details in Appendix B.2). The comparison highlights the
 351 advantage of our method in achieving accuracy while maintaining low complexity.

352 Figure 4a shows the top 10 brain edges based on regression analysis of denoised tensor from **NonparaT**
 353 against normalized IQ scores. We find that the top connections are mostly inter-hemisphere edges,
 354 consistent with recent research on brain connectivity [30, 35]. Figure 4b illustrates the results from
 355 NIPS data, where we plot the entries in $\hat{\Theta}$ corresponding to top authors and most-frequent words
 356 (after excluding generic words such as *figure*, *results*, etc). The identified pattern agrees with active
 357 topics in the NIPS publication. Among the top words are *neural* (marginal mean = 1.95), *learning*
 358 (1.48), and *network* (1.21), whereas top authors are *T. Sejnowski* (1.18), *B. Scholkopf* (1.17), *M.*
 359 *Jordan* (1.11), and *G. Hinton* (1.06). We also find strong heterogeneity among word occurrences
 360 across authors and years. For example, *training* and *algorithm* are popular words for *B. Scholkopf*
 361 and *A. Smola* in 1998-1999, whereas *model* occurs more often in *M. Jordan* and in 1996. The detected
 362 pattern and achieved accuracy demonstrate the applicability of our method.

363 6 Conclusion

364 We have developed a tensor estimation method that addresses both low- and high-rankness. Our sign
 365 series representation leads to nonparametric guarantees previously impossible. We hope the work
 366 opens up new inquiry that allows more researchers to contribute to this field.

References

- [1] Noga Alon, Shay Moran, and Amir Yehudayoff. Sign rank versus VC dimension. In *Conference on Learning Theory*, pages 47–80, 2016.
- [2] Pierre Alquier, Vincent Cottet, Guillaume Lécué, et al. Estimation bounds and sharp oracle inequalities of regularized procedures with lipschitz loss functions. *Annals of Statistics*, 47(4):2117–2144, 2019.
- [3] Animashree Anandkumar, Rong Ge, Daniel Hsu, Sham M Kakade, and Matus Telgarsky. Tensor decompositions for learning latent variable models. *Journal of Machine Learning Research*, 15(1):2773–2832, 2014.
- [4] Animashree Anandkumar, Rong Ge, and Majid Janzamin. Analyzing tensor power method dynamics in overcomplete regime. *Journal of Machine Learning Research*, 18(1):752–791, 2017.
- [5] Fadoua Balabdaoui, Cécile Durot, and Hanna Jankowski. Least squares estimation in the monotone single index model. *Bernoulli*, 25(4B):3276–3310, 2019.
- [6] Peter L Bartlett, Michael I Jordan, and Jon D McAuliffe. Convexity, classification, and risk bounds. *Journal of the American Statistical Association*, 101(473):138–156, 2006.
- [7] Changxiao Cai, Gen Li, H Vincent Poor, and Yuxin Chen. Nonconvex low-rank tensor completion from noisy data. In *Advances in Neural Information Processing Systems*, pages 1863–1874, 2019.
- [8] Stanley Chan and Edoardo Airoldi. A consistent histogram estimator for exchangeable graph models. In *International Conference on Machine Learning*, pages 208–216, 2014.
- [9] Eric C Chi, Brian J Gaines, Will Wei Sun, Hua Zhou, and Jian Yang. Provable convex co-clustering of tensors. *Journal of Machine Learning Research*, 21(214):1–58, 2020.
- [10] Henry Cohn and Christopher Umans. Fast matrix multiplication using coherent configurations. In *Proceedings of the twenty-fourth annual ACM-SIAM symposium on Discrete algorithms*, pages 1074–1087, 2013.
- [11] Lieven De Lathauwer, Bart De Moor, and Joos Vandewalle. A multilinear singular value decomposition. *SIAM Journal on Matrix Analysis and Applications*, 21(4):1253–1278, 2000.
- [12] Ronald De Wolf. Nondeterministic quantum query and communication complexities. *SIAM Journal on Computing*, 32(3):681–699, 2003.
- [13] Jicong Fan and Madeleine Udell. Online high rank matrix completion. In *Proceedings of the IEEE Conference on Computer Vision and Pattern Recognition*, pages 8690–8698, 2019.
- [14] Ravi Ganti, Nikhil Rao, Laura Balzano, Rebecca Willett, and Robert Nowak. On learning high dimensional structured single index models. In *Proceedings of the Thirty-First AAAI Conference on Artificial Intelligence*, pages 1898–1904, 2017.
- [15] Ravi Sastry Ganti, Laura Balzano, and Rebecca Willett. Matrix completion under monotonic single index models. In *Advances in Neural Information Processing Systems*, pages 1873–1881, 2015.
- [16] Martin Genzel and Alexander Stollenwerk. Robust 1-bit compressed sensing via hinge loss minimization. *Information and Inference: A Journal of the IMA*, 9(2):361–422, 2020.
- [17] Navid Ghadermarzy, Yaniv Plan, and Ozgur Yilmaz. Learning tensors from partial binary measurements. *IEEE Transactions on Signal Processing*, 67(1):29–40, 2018.
- [18] Navid Ghadermarzy, Yaniv Plan, and Özgür Yilmaz. Near-optimal sample complexity for convex tensor completion. *Information and Inference: A Journal of the IMA*, 8(3):577–619, 2019.

- [19] Amir Globerson, Gal Chechik, Fernando Pereira, and Naftali Tishby. Euclidean embedding of co-occurrence data. *Journal of Machine Learning Research*, 8:2265–2295, 2007.
- [20] Rungang Han, Rebecca Willett, and Anru Zhang. An optimal statistical and computational framework for generalized tensor estimation. *arXiv preprint arXiv:2002.11255*, 2020.
- [21] Trevor Hastie, Robert Tibshirani, and Jerome Friedman. *The elements of statistical learning: data mining, inference, and prediction*. Springer Science & Business Media, 2009.
- [22] Lifang He, Chun-Ta Lu, Guixiang Ma, Shen Wang, Linlin Shen, S Yu Philip, and Ann B Ragin. Kernelized support tensor machines. In *International Conference on Machine Learning*, pages 1442–1451. PMLR, 2017.
- [23] Christopher J Hillar and Lek-Heng Lim. Most tensor problems are NP-hard. *Journal of the ACM (JACM)*, 60(6):45, 2013.
- [24] Frank L Hitchcock. The expression of a tensor or a polyadic as a sum of products. *Journal of Mathematics and Physics*, 6(1-4):164–189, 1927.
- [25] David Hong, Tamara G Kolda, and Jed A Duersch. Generalized canonical polyadic tensor decomposition. *SIAM Review*, 62(1):133–163, 2020.
- [26] Victoria Hore, Ana Viñuela, Alfonso Buil, Julian Knight, Mark I McCarthy, Kerrin Small, and Jonathan Marchini. Tensor decomposition for multiple-tissue gene expression experiments. *Nature genetics*, 48(9):1094, 2016.
- [27] Prateek Jain and Sewoong Oh. Provable tensor factorization with missing data. In *Advances in Neural Information Processing Systems*, volume 27, pages 1431–1439, 2014.
- [28] Tamara G Kolda and Brett W Bader. Tensor decompositions and applications. *SIAM Review*, 51(3):455–500, 2009.
- [29] Chanwoo Lee and Miaoyan Wang. Tensor denoising and completion based on ordinal observations. In *International Conference on Machine Learning*, pages 5778–5788, 2020.
- [30] Yonghui Li, Yong Liu, Jun Li, Wen Qin, Kuncheng Li, Chunshui Yu, and Tianzi Jiang. Brain anatomical network and intelligence. *PLoS Comput Biol*, 5(5):e1000395, 2009.
- [31] Andrea Montanari and Nike Sun. Spectral algorithms for tensor completion. *Communications on Pure and Applied Mathematics*, 71(11):2381–2425, 2018.
- [32] Greg Ongie, Rebecca Willett, Robert D. Nowak, and Laura Balzano. Algebraic variety models for high-rank matrix completion. In *International Conference on Machine Learning*, pages 2691–2700, 2017.
- [33] Peter M Robinson. Root-N-consistent semiparametric regression. *Econometrica: Journal of the Econometric Society*, 56(4):931–954, 1988.
- [34] Clayton Scott. Surrogate losses and regret bounds for cost-sensitive classification with example-dependent costs. In *ICML*, 2011.
- [35] Lu Wang, Daniele Durante, Rex E Jung, and David B Dunson. Bayesian network–response regression. *Bioinformatics*, 33(12):1859–1866, 2017.
- [36] Miaoyan Wang and Lexin Li. Learning from binary multiway data: Probabilistic tensor decomposition and its statistical optimality. *Journal of Machine Learning Research*, 21(154):1–38, 2020.
- [37] Miaoyan Wang and Yuchen Zeng. Multiway clustering via tensor block models. In *Advances in Neural Information Processing Systems*, pages 713–723, 2019.
- [38] Ming Yuan and Cun-Hui Zhang. On tensor completion via nuclear norm minimization. *Foundations of Computational Mathematics*, 16(4):1031–1068, 2016.
- [39] Anru Zhang and Dong Xia. Tensor SVD: Statistical and computational limits. *IEEE Transactions on Information Theory*, 64(11):7311 – 7338, 2018.

Checklist

1. For all authors...

- (a) Do the main claims made in the abstract and introduction accurately reflect the paper's contributions and scope? [Yes] See Section 1, **Our contributions**.
- (b) Did you describe the limitations of your work? [Yes] Theoretical assumptions and limitations are described in Sections 3.2 and 4.1. Numerical assumptions are stated in Section 5.
- (c) Did you discuss any potential negative societal impacts of your work? [N/A] This work does not present any foreseeable societal consequence.
- (d) Have you read the ethics review guidelines and ensured that your paper conforms to them? [Yes]

2. If you are including theoretical results...

- (a) Did you state the full set of assumptions of all theoretical results? [Yes] The assumptions for main Theorems are fully stated in Sections 3.2 and 4.1. The assumptions for Theorem 4 and technical lemmas are stated in Appendix A.
- (b) Did you include complete proofs of all theoretical results? [Yes] All proofs are provided in Appendix A. Short proof intuition is provided in Section 2. Comparison with existing theory is provided in Sections 3 and 4.1.

3. If you ran experiments...

- (a) Did you include the code, data, and instructions needed to reproduce the main experimental results (either in the supplemental material or as a URL)? [Yes] See Section 5 and Appendix C. Code and user manual are submitted as supplemental materials.
- (b) Did you specify all the training details (e.g., data splits, hyperparameters, how they were chosen)? [Yes] Training procedures are described in Section 5. Additional details on hyperparameter selection and cross validation results are provided in Appendix C.
- (c) Did you report error bars (e.g., with respect to the random seed after running experiments multiple times)? [Yes] Error bars are provided in all Figures/Tables in the main paper and in Appendix C.
- (d) Did you include the total amount of compute and the type of resources used (e.g., type of GPUs, internal cluster, or cloud provider)? [Yes] Computational platform and running time are detailed in Appendix C.

4. If you are using existing assets (e.g., code, data, models) or curating/releasing new assets...

- (a) If your work uses existing assets, did you cite the creators? [Yes] Data source has been cited in Section C, **Data applications**.
- (b) Did you mention the license of the assets? [N/A] No license available for the assets used in this work.
- (c) Did you include any new assets either in the supplemental material or as a URL? [Yes] We have submitted the software package as supplemental materials.
- (d) Did you discuss whether and how consent was obtained from people whose data you're using/curating? [N/A] The datasets are publicly available.
- (e) Did you discuss whether the data you are using/curating contains personally identifiable information or offensive content? [N/A] No personally identifiable information is included in the datasets.

5. If you used crowdsourcing or conducted research with human subjects...

- (a) Did you include the full text of instructions given to participants and screenshots, if applicable? [N/A] This work does not involve human subjects.

- 504 (b) Did you describe any potential participant risks, with links to Institutional Review
505 Board (IRB) approvals, if applicable? [N/A] This work does not involve potential
506 participant risk.
- 507 (c) Did you include the estimated hourly wage paid to participants and the total amount
508 spent on participant compensation? [N/A] This work does not involve participants.